

# A Strain-engineered Helical Structure as a Self-adaptive Magnetic Microswimmer

Xiaojie Shi,<sup>[a]</sup> Jinrun Liu,<sup>[a]</sup> Ye Kong,<sup>[a]</sup> Borui Xu,<sup>\*,[a]</sup> Tianlong Li,<sup>\*,[b]</sup> Alexander A. Solovev,<sup>[a]</sup> and Yongfeng Mei<sup>\*,[a]</sup>

**Abstract:** Inspired by flagellar bacteria, helical microswimmers are proposed in many biomedical applications due to their efficient propulsion at low Reynolds numbers. And the ability to swim through a confined environment such as a blood capillary is an urgent issue to further expand their functions both *in vivo* and *in vitro*. Herein, we report an inorganic but soft helical microswimmer that can accurately navigate and achieve self-adaptive locomotion driven by a weak magnetic field. The microswimmer is made via nano-

membrane self-rolling method. The motion of helical microswimmer is influenced by its structures such as size and pitch, which can be precisely manipulated by strain engineering during fabrication. Self-adaptive motion is demonstrated in a confined capillary filled with viscous fluid. This helical microswimmer is expected as a magnetic microtool applied to thrombosis treatment as a combination of rigid inorganic materials and soft helical structure.

## Introduction

In nature, bacteria can exploit flagellar mechanism to swim in low-Reynolds-number liquid.<sup>[1,2]</sup> The Reynolds number is defined as the ratio of inertial forces to viscous force as follows:  $Re = \rho v l / \mu$ , where  $\rho$ ,  $v$ ,  $l$ ,  $\mu$  are the density of the fluid, the velocity of the fluid relative to the moving body, the characteristic length of the body, and the dynamic viscosity of the fluid, respectively. In low-Reynolds-number flow, the object is in a world which is very small and vicious, that is, once the propelled force disappears, the movement stops immediately. Inspired by this, artificial flagella-like microswimmers were reported, which are wirelessly controlled to swim under magnetic field.<sup>[3,4,5,6]</sup> These magnetic helical microswimmers have been extensively used *in vivo* tasks as targeted drug delivery,<sup>[7]</sup> sensing,<sup>[8]</sup> diagnosis,<sup>[9]</sup> and micro-invasive surgery.<sup>[10,11]</sup> Considering the complex environment in human body, these microswimmers also require adaptive motion as the ability to cross biological barriers and move through blood vessels. Recently, a helical microswimmer made of polymers with magnetic nanoparticles realizes adaptive locomotion due to its low rigidity.<sup>[12]</sup> However, considering that the magnetic forces and torques are proportional to the

volume of magnetic materials, propulsion efficiency of these soft polymer microswimmers is relatively low due to the limited loading amount of magnetic component.<sup>[13,14,15]</sup> Instead, this drawback can be overcome once the microswimmer is made of totally inorganic parts, while the ability of adaptive motion becomes a problem because of the loss of softness.

In this work, we report a soft magnetic helical microswimmer consisting of inorganic nanomembranes, which is fabricated by rolled-up nanotechnology.<sup>[16,17]</sup> Nanomembrane with pre-layer internal strain rolls up with the intercalation of liquid that allows us to design and fabricate microhelices in various shapes through strain engineering.<sup>[18]</sup> In a rotating magnetic field, the helical microswimmer generates corkscrew motion in viscous fluid. We find that the speed of helical microswimmer is influenced by surrounding environments and structure parameters. Moreover, the strong magnetic torque generated by the all-magnetic structure allows it to overcome high viscous resistance and navigate in human blood vessels. Our rolled-up helical microswimmer driven by rotating magnetic field fills in the gap between rigid microswimmers and soft ones. Ag/Ti/Ni microswimmer has exceptionally high degrees of flexibility which can be dynamically driven to the desired position due to the adaptive motion capability. At the same time, the microswimmer with a shape tip can work at high frequency and remain stable on the thrombus surface to cutting and drilling operation.<sup>[19]</sup> Therefore, the microswimmer is expected to disperse thrombus through drilling operation.

## Results and Discussion

Magnetic microswimmer was fabricated by nanomembrane self-rolling strategy.<sup>[20,21,22]</sup> Figure 1a schematically shows that the nanomembrane rolled into a helix by strain-engineering. Firstly, the shadow mask was covered on a cleaned glass substrate, as displayed in Figure 1a-l. Then, pre-strained metal

[a] X. Shi, J. Liu, Y. Kong, Dr. B. Xu, Prof. A. A. Solovev, Prof. Y. Mei  
Department of Materials Science & State Key Laboratory of ASIC and Systems  
Fudan University, 220 Handan Road, Shanghai 200433 (P. R. China)  
E-mail: xuborui@fudan.edu.cn  
yfm@fudan.edu.cn

[b] Prof. T. Li  
School of Mechatronics Engineering & State Key Laboratory of Robotics and System  
Harbin Institute of Technology, 92 Xi Da Zhi Jie, Haerbin 150001 (P. R. China)  
E-mail: tianlongli@hit.edu.cn

Supporting information for this article is available on the WWW under <https://doi.org/10.1002/cnma.202100055>

This manuscript is part of a special collection: "Beyond Active Colloids: From Functional Materials to Microscale Robotics".

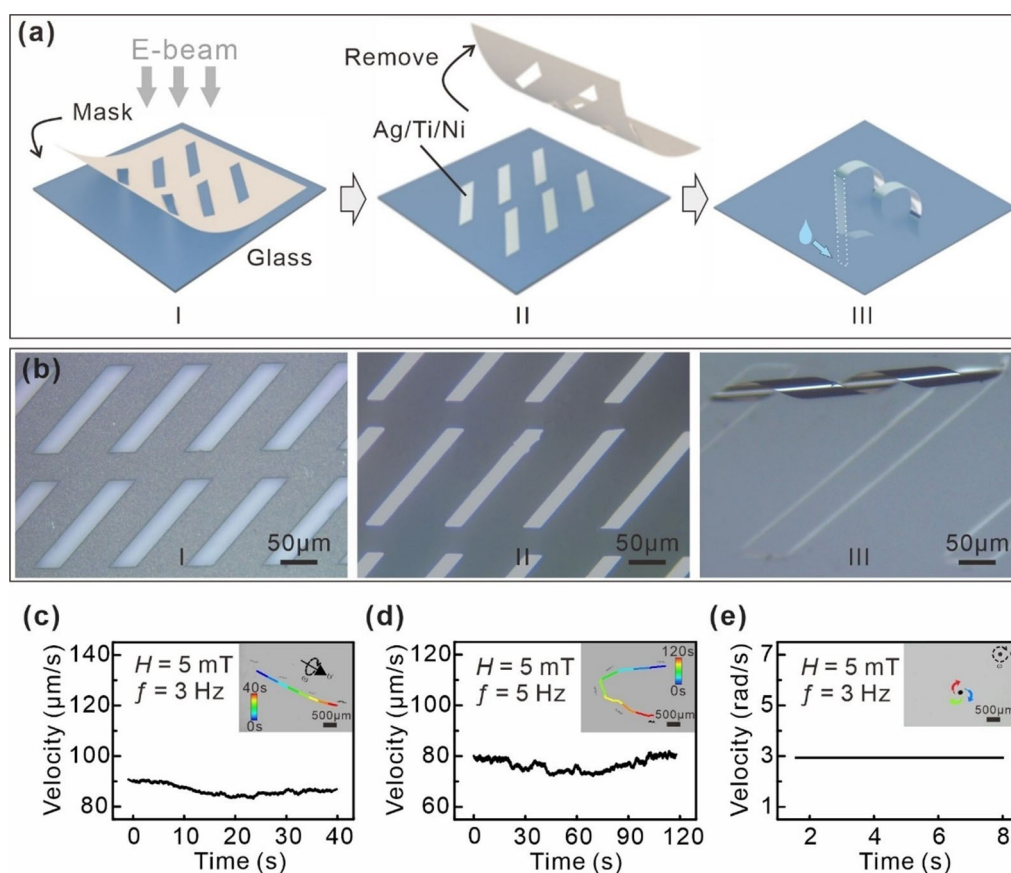


**Figure 1.** Fabrication and swimming behavior of microswimmers. (a) Schematic diagram of the preparation process. I represents mask covering and nanomembrane deposition. II represents mask removing after deposition. III represents deposited nanomembrane rolls into helical structure after liquid contact. (b) Optical microscope pictures of fabrication process. I shows the substrate covered by a shadow mask. II is the deposited nanomembranes after mask removing. III is a resultant helical microstructure. (c–e) Instantaneous velocity of microswimmer. (c) forward locomotion. (d) steering locomotion. (e) vertical rotation. Insets are the time-lapse image showing a microswimmer swimming in three dimensions in viscous fluid. The rainbow line is the moving trajectory of microswimmer. The phantom is the posture and position of the microswimmer in the previous time.  $\omega$  and  $v$  stands for the rotating directions of the magnetic field of magnetic field and swimming directions, respectively.

nanomembrane consisting of Ag, Ti, and Ni was deposited onto the substrate by electron beam evaporation. After deposition, the shadow mask was removed, leaving the ordered parallelogram nanoarrays (Figure 1a-II). Finally, we used microoperation to drop a droplet of alcohol on the surface. When the droplet touched the nanomembrane, it triggered the rolling behavior of the parallelogram-patterned nanomembrane. The liquid continued to diffuse between the substrate and the nanomembrane until the curling was completed. As a result, the parallelogram-patterned metal layers rolled up in a helical scroll (Figure 1a-III). Here, the materials of the nanomembrane were selected for different purposes. Ag layer was applied to generate van der Waals interaction with the substrate. Ti and Ni layers were deposited to generate strain gradients as well as magnetic function. Figure 1b shows the optical images of the preparation process corresponding to Figure 1a. Figure 1b-I shows the result after covering the mask. An array of parallelogram-patterned Ag/Ti/Ni nanomembrane are constructed by electron beam evaporation as shown in Figure 1b-II. Figure 1b-III shows a helical microstructure of Ag/Ti/Ni on the substrate.

Figures 1c to 1e show the swimming performance of a microswimmer in viscous fluid, in which a rotating magnetic field of 5 mT was applied. In Figure 1c, the microswimmer maintains a linear motion with a steady velocity of approximately  $86 \mu\text{m s}^{-1}$ . And in Figure 1d, the velocity is about  $74 \mu\text{m s}^{-1}$ . For vertical rotation, the microswimmer rotates synchronously with the magnetic field, fixing at 3 rad  $\text{s}^{-1}$  as shown in Figure 1e. Thus, the swimming speed of a helical microswimmer is basically stable under a fixed magnetic field strength and frequency. The change of microswimmer movement position with time is shown by the colorful line in the figure, and the phantom is the posture and position of the microswimmer in the previous time. These images confirm that the magnetic helical microswimmer can perform navigation in different manners under designed rotating magnetic fields. Figure 1c shows that the microswimmer performs corkscrew and drift motion as it advances from left to right. (movie S1) And Figure 1d shows that the moving direction of microswimmer is controlled precisely by simply changing the rotating axis of the magnetic field. (movie S2) In addition, the microswimmer swims vertically in Figure 1e. (movie S3) These results

show that the locomotion of microswimmer could be well-controlled under external magnetic field with elaborate design. The propulsion force of microswimmer comes from the magnetization of magnetic Ni layer as exposed in a uniform magnetic field. So the microswimmer rotates as placed in a rotating magnetic field, resulting in a translational movement which makes the microswimmer move forward. With changing the axis of the magnetic field to the z axis, the magnetization direction of the helical microswimmer is still along the long axis, and the orientation of the long axis was adjusted in the liquid to be consistent with the magnetic field to obtain vertical motion.<sup>[23]</sup> Since the increase of viscous resistance near the solid boundary, a resistant torque is exerted to the microswimmer causing drift.<sup>[24]</sup>

As the nanomembrane self-rolling is driven by the internal strain and triggered by the intercalation of liquid, we can design and fabricate the helices in various shapes through strain-engineering and liquid contact.<sup>[25]</sup> The parameters designed to control the resultant structure are shown in Figure 2a. Strain engineering is applied through altering the deposition parameters as nanomembrane's thickness. The liquid contact is tuned through three parameters, which are defined as the trigger distance ( $d$ ), the pattern's interior angle ( $\theta$ ), and the rolling angle ( $\phi$ ). Here, the rolling angle ( $\phi$ ) is the angle between the rolling direction and the long side of the parallelogram pattern.

Figure 2b investigates the relationship between deposition total thickness and helix diameter, in which the thicknesses of Ag, Ti and Ni layers are the same. According to the elastic mechanism,<sup>[26]</sup> the diameter of self-rolling nanomembrane is positively correlated with the total thickness as the thickness of each layer is equal, as depicted by the red line in Figure 2b. The result reflects that the size of helical microstructure can be well controlled in deposition process. Besides, Figure 2c shows the relationship between the rolling angle ( $\phi$ ) and the trigger distance ( $d$ ). As the trigger distance changes, the nanomem-

brane rolls from the trigger position to different directions, resulting in different helix pitches. The rolling angle increases with the trigger distance moving away from the bottom corner, and there is a simple linear relationship between  $\theta$  and  $d$  as the fitting blue line in Figure 2c. Furthermore, a series of parallelogram patterns with different interior angles are designed as 30°, 45°, 60° and 75° to explore the influence of the interior angle on the resultant structures. We find that the pitch of the helix rapidly decreases and slowly flattens as the interior angle of the parallelogram nanomembrane increases. Therefore, the design of 3D helical microswimmer prepared by self-rolling of the nanomembrane are manipulated by three factors, including the total thickness of metal layers, the patterning size of the nanomembrane, and the droplet trigger point of the long side. By adjusting the three structural parameters, different helical structures can be obtained.

Figure 3 shows wirelessly controlled swimming performance of microswimmers in liquid. In this part, the magnetic field strength is 5 mT. The results indicate that the microswimmer's velocity increases linearly with frequency at low frequency, as expected in the low-Reynolds-number environment.<sup>[27]</sup> After reaching a maximum velocity, the velocity reduces with increasing field frequency and the swimming movement becomes unstable. (Figure S1) When the frequency increases to a certain value, the helical microswimmer remains stationary, neither rotating nor moving. The corresponding frequency at the maximum velocity is called step-out frequency.<sup>[28,29]</sup>

The shape and structure of the helical microswimmer also dramatically affect the performance of swimming.<sup>[30,31]</sup> Firstly, the influence of helical pitch was investigated as shown in Figure 3a. For the same pattern, the nanomembrane will preferentially release from the substrate at the contact position of the droplet and the nanomembrane and roll up into the final structure. These helices are made from the same pattern with the same volume of magnetic layers, while the rolling direction is tuned by the liquid contact point. In the top panel in Figure 3a, there is a step in velocity due to a long-distance drifting or jumping movement. The reason is that intricate changes in hydrodynamics during high-frequency rotation effects sudden increase in drift speed. It is concluded that the swimming velocity tends to increase first and then decrease as the pitch changes. The microswimmer with the pitch set as 300  $\mu\text{m}$  seems to be a preferable pitch of the helix among them, of which the helix angle is 55°.<sup>[32]</sup>

The step-out frequency is also largely influenced by the helical pitch and helical angle, which decreases with the helical pitch increasing. Moreover, the length of the nanomembrane pattern is controlled to construct microhelices with different lengths, and corresponding performance is shown in Figure 3b. The microswimmer was propelled through the difference in resistance between a slender body normal and parallel to the slender direction as it is pulled through fluid. Resistance torque is affected by helical angle and the magnetic torque is affected the volume of magnetic material. In a rotating magnetic field with the same magnitude, the step-out frequency and the maximum velocity of helical microswimmer increase with the reduction of body length, which is attributed to the competi-

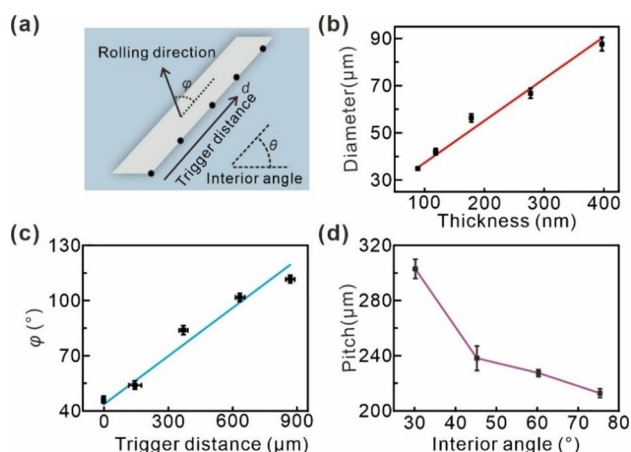


**Figure 2.** Shape factor effect on the rolling behavior. (a) Schematic diagram of shape factors including trigger distance  $d$ , rolling direction  $\phi$ , and interior angle  $\theta$ . (b) Helix diameter as a function of total thickness. Red line depicts the fitting curve. (c) Rolling direction ( $\phi$ ) as a function of trigger distance ( $d$ ). Blue line is the fitting curve. (d) Helix pitch as a function of interior angle ( $\theta$ ).

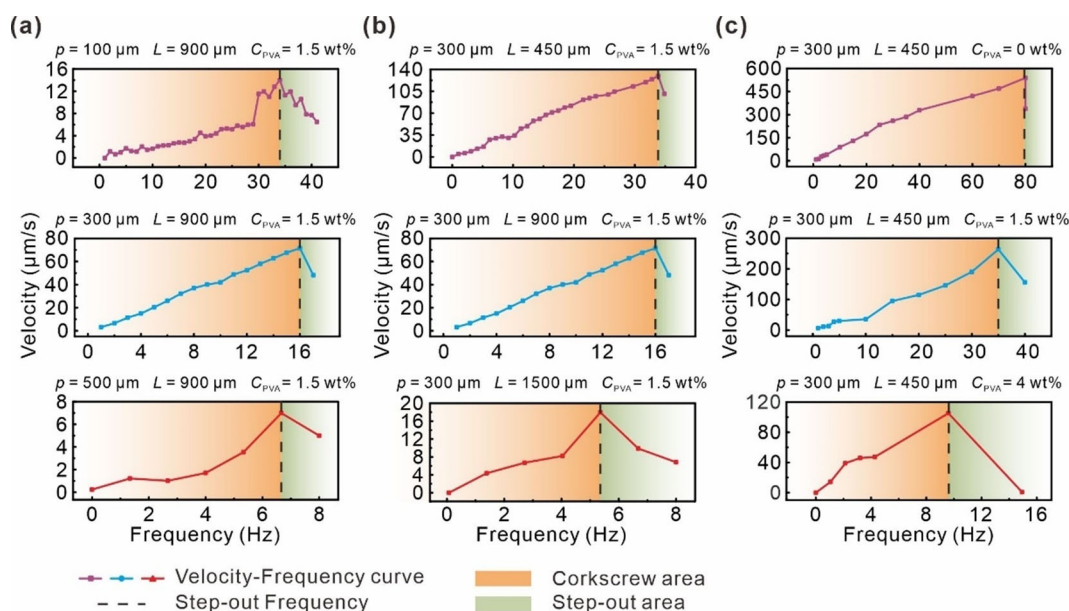


**Figure 3.** Wirelessly controlled swimming performance of microswimmer in liquid. (a) Dependence of microswimmer velocity on the helix pitch ( $p$ ). (b) Dependence of microswimmer velocity on the pattern length ( $L$ ). (c) Dependence of microswimmer velocity on the liquid viscosity ( $C_{PVA}$ ). The strength of the magnetic field is 5 mT.

tion between the magnetic torque and resistance torque in swimming process.<sup>[33]</sup> According to the previous discussion, the helical microswimmer with optimal performance was further tested in the fluid with different viscosities as shown in Figure 3c. In fluid with the viscosity similar to blood ( $C_{PVA} = 1.5 \text{ wt}\%$ ), the step-out frequency is 38 Hz, lower than that in water. Such swimming performance exceeds the maximum velocity and step-out frequency of organic helical magnetic microswimmers<sup>[34]</sup> and the microswimmer with a thin Ni square

plate as a “head” and a nonmagnetic “tail”.<sup>[35]</sup> And this promotion can be attributed to the enhanced magnetic torque due to increased loading ratio of magnetic part.

Furthermore, it is of great importance to investigate the ability of adaptive motion in a confined environment as microswimmers are usually expected to be applied in a blood vessel.<sup>[36]</sup> In Figure 4a, the microswimmer swims forward stably without drifting in a thin glass capillary with 500 μm diameter, in which magnetic field with 5 mT strength is applied.

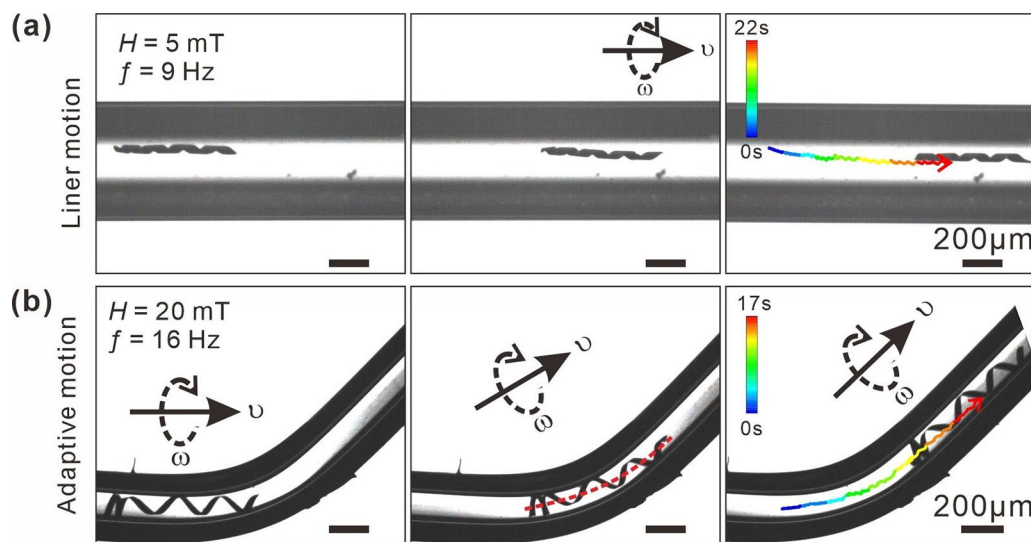


**Figure 4.** Time-lapse images of the helical microswimmer actuated by the rotating magnetic field in the water-filled narrow straight capillary channel in 500 μm diameter (a) and the curved tube in 300 μm diameter (b) under the full magnetic field. The red line is the long axis of the helical microswimmer. The rainbow line is the moving trajectory of microswimmer.

(movie S4) The microswimmer is affected by multifaceted tri-dimensional boundaries in a closed environment. Thus, the contact force brought from the boundaries cancels each other, leading to a directional motion without drifting.<sup>[37]</sup> Figure 4b shows the microswimmer goes through a narrow curved capillary in 20 mT rotating magnetic field. The red line depicts the variation in axial direction due to the difference in obstruction experienced by different parts of the body. Simultaneously, the microswimmer moves forward with cork-screw rotation in the rotating magnetic field. (movie S5) After the microswimmer pass through the curved region, it regains its original shape which means the whole deformation is elastic. The realization of such adaptive motion reflects that our helical microswimmer has a relatively low equivalent bending stiffness while it is made of rigid inorganic materials, which is further confirmed in Figure S2.

## Conclusion

In summary, an inorganic helical microswimmer with considerable magnetic loading is fabricated through electron beam evaporation and self-rolling nanotechnology. We present a strain-engineering method and design several parameters for the modulation of shapes, which includes deposition thickness, trigger distance, and pattern's internal angle. All helical microswimmers perform effective motion with rotating magnetic field below their step-out frequencies. It is noticed that an optimal pitch should exist, and in our experiment, a pitch of approximately 300  $\mu\text{m}$  and the helix angle of approximately 55° results in a maximum velocity. Meanwhile, smaller size has better swimming performance due to the less resistance torque. Our helical microswimmer can be propelled at high velocity in viscosity aqueous environment, which indicates great promise for future biomedical applications. Through reducing pattern size and film thickness flexibly, small helical microswimmers will be obtained, which are completely suitable for human blood vessels.<sup>[38]</sup> Also, the realization of adaptive motion due to its soft helical microstructure broadens its potential *in vivo* applications. With further functionalization strategies, we believe that this helical magnetic microswimmer reaching the balance between rigid and soft will be used in targeted drug delivery and disperse thrombus.

## Experimental Section

**Fabrication of helical microswimmers:** Firstly, a glass substrate was cleaned by ultrasonication in DI water, ethanol, and acetone solution, separately. A shadow mask with parallelogram cells was pasted on the glass substrate. Then, a multilayer nanomembrane consisting of Ag, Ti, and Ni was deposited on the substrate by electron beam evaporation, and its thickness was adjusted to be equal for each layer. The deposition rates of Ag, Ni, and Ti layers were 0.15  $\text{nm s}^{-1}$ , 0.2  $\text{nm s}^{-1}$ , and 0.25  $\text{nm s}^{-1}$ , respectively. After depositing these three layers and removing the mask, a parallelogram nanomembrane array was obtained on the glass substrate. Then, a tip of capillary containing ethanol was placed on the surface. Due to the capillary force and surface tension, a small

amount of ethanol was dispersed between the substrate and the capillary. When the microdroplets touched the nanomembrane, the nanomembrane started to roll up from the contact point. By controlling the capillary through a micromanipulator, the droplet on the surface of the substrate was controlled to precisely manipulate the rolling behavior of the parallelogram-nanomembranes.

**Preparation of micropool:** The micropool was made of PDMS. To prepare the micropool, the base and curing agent were mixed evenly at a ratio of 10:1 into a glass dish. After vacuum degassing, the system was heated it at 150 degrees Celsius for 15 minutes. Then a 5 cm  $\times$  2 cm area was carved out.

**Recording of swimming performance:** Helmholtz device composed of three pairs of orthogonal coils was used to generate rotating magnetic field for swimming test. A micromanipulator was used to control the tip of the capillary to pick up and release the fabricated microswimmer into the PDMS micropool, which was filled with the Pseudo biological solution. The solution is polyvinyl alcohol (PVA) aqueous solution with 0.48 wt% sodium dodecyl benzene sulfonate (SDBS). The size of micropool was 5 cm  $\times$  2 cm. The micropool was placed in the center of the Helmholtz setting to ensure the uniformity of the magnetic field. A rotating magnetic field with certain strength was applied to perform a swimming test on the manufactured magnetic helical microswimmers. The motion of microswimmer was recorded by a CCD camera connected with an optical microscope in 22.5 fps. TrackMate<sup>[39]</sup> from the image processing software Fiji was used for microswimmer tracking to obtain the trajectory data. For adaptive motion test, a curved capillary channel with desired angle is prepared by heating and bending through a needle puller. The solution and the microswimmer was inhaled in the capillary through the micromanipulator with a syringe.

## Acknowledgements

This work is supported by the Natural Science Foundation of China (Nos. 61975035, 62005050, 51961145108, 51850410502, 51705108), Program of Shanghai Academic Research Leader (19XD1400600).

## Conflict of Interest

The authors declare no conflict of interest.

**Keywords:** Helical microswimmer · adaptive motion · magnetic propulsion · strain engineering · nanomembrane

- [1] E. M. Purcell, *Am. J. Phys.* **1977**, *45*, 3.
- [2] E. Lauga, *Annu. Rev. Fluid Mech.* **2016**, *48*, 105.
- [3] A. Ghosh, P. Fischer, *Nano Lett.* **2009**, *9*, 2243.
- [4] L. Zhang, J. J. Abbott, L. X. Dong, B. E. Kratochvil, D. Bell, B. J. Nelson, *Appl. Phys. Lett.* **2009**, *94*, 3.
- [5] J. J. Abbott, K. E. Peyer, M. C. Lagomarsino, L. Zhang, L. X. Dong, I. K. Kaliakatsos, B. J. Nelson, *Int. J. Robot. Res.* **2009**, *28*, 1434.
- [6] L. Zhang, J. J. Abbott, L. X. Dong, K. E. Peyer, B. E. Kratochvil, H. X. Zhang, C. Bergeles, B. J. Nelson, *Nano Lett.* **2009**, *9*, 3663.
- [7] F. Qin, Y. Zhang, F. Peng, *ChemNanoMat.* **2021**, <https://doi.org/10.1002/cnma.202000647>

- [8] O. Ergeneman, G. Dogangil, M. P. Kummer, J. J. Abbott, M. K. Nazeeruddin, B. J. Nelson, *IEEE Sens. J.* **2008**, *8*, 29.
- [9] X. H. Yan, Q. Zhou, M. Vincent, Y. Deng, J. F. Yu, J. B. Xu, T. T. Xu, T. Tang, L. M. Bian, Y. X. J. Wang, K. Kostarelos, L. Zhang, *Sci. Robot.* **2017**, *2*, 14.
- [10] B. J. Nelson, I. K. Kaliakatsos, J. J. Abbott, *Annu. Rev. Biomed. Eng.* **2010**, *12*, 55.
- [11] X.-Z. Chen, J.-H. Liu, M. Dong, L. Mueller, G. Chatzipirpiridis, C. Hu, A. Terzopoulou, H. Torlakcik, X. Wang, F. Mushtaq, J. Puigmarti-Luis, Q.-D. Shen, B. J. Nelson, S. Pane, *Mater. Horiz.* **2019**, *6*, 1512.
- [12] H. W. Huang, F. E. Uslu, P. Katsamba, E. Lauga, M. S. Sakar, B. J. Nelson, *Sci. Adv.* **2019**, *5*, eaau1532.
- [13] M. Dong, X. Wang, X.-Z. Chen, F. Mushtaq, S. Deng, C. Zhu, H. Torlakcik, A. Terzopoulou, X.-H. Qin, X. Xiao, J. Puigmarti-Luis, H. Choi, A. P. Pego, Q.-D. Shen, B. J. Nelson, S. Pane, *Adv. Funct. Mater.* **2020**, *30*, 1910323.
- [14] X. Wang, X.-H. Qin, C. Hu, A. Terzopoulou, X.-Z. Chen, T.-Y. Huang, K. Maniura-Weber, S. Pane, B. J. Nelson, *Adv. Funct. Mater.* **2018**, *28*, 1804107.
- [15] K. Kamata, Z. Piao, S. Suzuki, T. Fujimori, W. Tajiri, K. Nagai, T. Iyoda, A. Yamada, T. Hayakawa, M. Ishiwara, S. Horaguchi, A. Belay, T. Tanaka, K. Takano, M. Hangyo, *Sci. Rep.* **2014**, *4*, 4919.
- [16] Z. Chen, G. S. Huang, I. Trase, X. M. Han, Y. F. Mei, *Phys. Rev. Appl.* **2016**, *5*.
- [17] G. S. Huang, Y. F. Mei, *J. Materiomics* **2015**, *1*, 296.
- [18] Y. Mei, G. Huang, A. A. Solovev, E. B. Urena, I. Moench, F. Ding, T. Reindl, R. K. Y. Fu, P. K. Chu, O. G. Schmidt, *Adv. Mater.* **2008**, *20*, 4085.
- [19] W. Xi, A. A. Solovev, A. N. Ananth, D. H. Gracias, S. Sanchez, O. G. Schmidt, *Nanoscale* **2013**, *5*, 1294.
- [20] Z. Tian, W. Huang, B. R. Xu, X. L. Li, Y. F. Mei, *Nano Lett.* **2018**, *18*, 3688.
- [21] G. S. Huang, Y. F. Mei, *Small* **2018**, *14*, 1703665.
- [22] B. Xu, X. Zhang, Z. Tian, D. Han, X. Fan, Y. Chen, Z. Di, T. Qiu, Y. Mei, *Nat. Commun.* **2019**, *10*, 5019.
- [23] K. E. Peyer, L. Zhang, B. J. Nelson, *Appl. Phys. Lett.* **2011**, *99*, 174101.
- [24] L. Zhang, J. J. Abbott, L. Dong, K. E. Peyer, B. E. Kratochvil, H. Zhang, C. Bergeles, B. J. Nelson, *Nano Lett.* **2009**, *9*, 3663.
- [25] B. R. Xu, B. R. Zhang, L. Wang, G. S. Huang, Y. F. Mei, *Adv. Funct. Mater.* **2018**, *28*, 1705872.
- [26] G. P. Nikishkov, *J. Appl. Phys.* **2003**, *94*, 5333.
- [27] P. Fischer, A. Ghosh, *Nanoscale* **2011**, *3*, 557.
- [28] A. Cho, *Sci. J.* **2006**, *313*, 164.
- [29] T. Honda, K. I. Arai, K. Ishiyama, *IEEE Trans. Magn.* **1996**, *32*, 5085.
- [30] S. Tottori, L. Zhang, F. Qiu, K. K. Krawczyk, A. Franco-Obregon, B. J. Nelson, *Adv. Mater.* **2012**, *24*, 811.
- [31] K. I. Morozov, A. M. Leshansky, *Nanoscale* **2014**, *6*, 12142.
- [32] R. Valdes, V. Angeles, E. de la Calleja, R. Zenit, *Phys. Rev. Fluids* **2019**, *4*, 084302.
- [33] D. Gong, J. Cai, N. Celi, L. Feng, Y. Jiang, D. Zhang, *J. Magn. Magn. Mater.* **2018**, *468*, 148.
- [34] W. Gao, X. M. Peng, A. Pei, C. R. Kane, R. Tam, C. Hennessy, J. Wang, *Nano Lett.* **2014**, *14*, 305.
- [35] L. Zhang, K. E. Peyer, B. J. Nelson, *Lab Chip* **2010**, *10*, 2203.
- [36] H.-W. Huang, M. S. Sakar, A. J. Petruska, S. Pane, B. J. Nelson, *Nat. Commun.* **2016**, *7*, 12263.
- [37] E. Lauga, W. R. DiLuzio, G. M. Whitesides, H. A. Stone, *Biophys. J.* **2006**, *90*, 400.
- [38] A. A. Solovev, Y. Mei, Ureña, E. Bermúdez, G. Huang, O. G. Schmidt, *Small* **2009**, *5*, 1688.
- [39] K. Jaqaman, D. Loerke, M. Mettlen, H. Kuwata, S. Grinstein, S. L. Schmid, G. Danuser, *Nat. Methods* **2008**, *5*, 695.

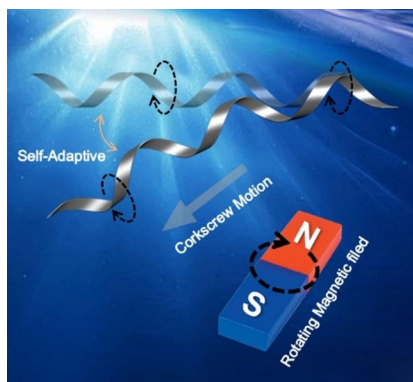
Manuscript received: January 29, 2021

Revised manuscript received: February 27, 2021

Version of record online: ■■■, ■■■■

## FULL PAPER

An inorganic helical microswimmer with both flexibility and rigidity has been fabricated by a strain-engineering method. It performs an effective corkscrew and self-adaptive motion in a rotating magnetic field.



*X. Shi, J. Liu, Y. Kong, Dr. B. Xu\*,  
Prof. T. Li\*, Prof. A. A. Solovev, Prof. Y.  
Mei\**

1 – 7

**A Strain-engineered Helical  
Structure as a Self-adaptive  
Magnetic Microswimmer**

